Asian Zika virus strains target CD14+ blood monocytes and induce M2-skewed immunosuppression during pregnancy

Suan-Sin Foo[1], Weiqiang Chen[1], Yen Chan[2], James W. Bowman[1], Lin-Chun Chang[1], Younho Choi[1], Ji Seung Yoo[1], Jianning Ge[1], Genhong Cheng[3], Alexandre Bonnin[4], Karin Nielsen-Saines[5], Patrícia Brasil[6] and Jae U. Jung [1]*

Blood CD14+ monocytes are frontline immunomodulators categorized into classical, intermediate or non-classical subsets, and subsequently differentiated into M1 pro- or M2 anti-inflammatory macrophages on stimulation. Although the Zika virus (ZIKV) rapidly establishes viraemia, the target cells and immune responses, particularly during pregnancy, remain elusive. Furthermore, it is unknown whether African- and Asian-lineage ZIKV have different phenotypic impacts on host immune responses. Using human blood infection, we identified CD14+ monocytes as the primary target for African- or Asian-lineage ZIKV infection. When immunoprofiles of human blood infected with ZIKV were compared, a classical/intermediate monocyte-mediated M1-skewed inflammation by the African-lineage ZIKV infection was observed, in contrast to a non-classical monocyte-mediated M2-skewed immunosuppression by the Asian-lineage ZIKV infection. Importantly, infection of the blood of pregnant women revealed an enhanced susceptibility to ZIKV infection. Specifically, Asian-lineage ZIKV infection of pregnant women's blood led to an exacerbated M2-skewed immunosuppression of non-classical monocytes in conjunction with a global suppression of type I interferon-signalling pathway and an aberrant expression of host genes associated with pregnancy complications. Also, 30 ZIKV+ sera from symptomatic pregnant patients showed elevated levels of M2-skewed immunosuppressive cytokines and pregnancy-complication-associated fibronectin-1. This study demonstrates the differential immunomodulatory responses of blood monocytes, particularly during pregnancy, on infection with different lineages of ZIKV.

Climate change and global warming have increased the toll of mosquito-borne diseases, due to development of favorable meteorological conditions for mosquito breeding[1]. Similar to other mosquito-borne flaviviruses such as Dengue virus, ZIKV is also transmitted by *Aedes* mosquitoes that are widely spread in most parts of the world[2]. Currently, ZIKV outbreaks have been reported in 59 countries, mainly affecting the North and South America continents[3]. Despite mild symptomatic illness being exhibited by only 20% of infected individuals, ZIKV has been unexpectedly associated with almost 3,000 cases of microcephaly and/or central nervous system malformations reported in 29 countries[3]. When ZIKV re-emerged on Yap Island in 2007, it appeared to have evolved from the original African lineage first discovered back in 1947 in Uganda, taking a new form, now identified as the Asian lineage[4,5]. Despite a 90% sequence homology between the two lineages, stark differences in the replication kinetics, infectivity and immune responses have been reported during infection of neural cells[6]. Recent advances on ZIKV have shed insights on its tropism for the maternal-fetal interface. ZIKV has been detected in placental tissues of infected expectant mothers, specifically within the placental macrophages, known as Hofbauer cells and intervillous histiocytes found on the maternal side[7,8]. Additionally, the neurotropism of ZIKV for glial cells and endothelial cells of fetal brains has also been identified[8].

Pregnancy is a sophisticated immune-altering process that requires prudent immunomodulation of the innate immunity to ensure healthy pregnancy outcomes[9]. In particular, circulating maternal monocytes play a crucial role as the activation and transition of monocytes to macrophages is essential for healthy placental development[10,11]. Blood monocytes exhibit morphological and functional plasticity that can be categorized into: (1) classical (CD14hi CD16− (CD, cluster of differentiation)), (2) intermediate (CD14hi CD16+) and (3) non-classical (CD14lo CD16+) subsets[12]. In addition, monocytes can differentiate further into pro-inflammatory M1 or anti-inflammatory M2 macrophages[11,13]. Although the fate of these monocyte subsets remains a subject of debate, findings from a mouse model of vascular inflammation suggest that classical and non-classical monocytes are most likely to differentiate into M1 and M2 macrophages, respectively[14]. During pregnancy, the continuous growth of the semi-allogeneic fetus in the expectant mother leads to an expansion of an intermediate monocyte population and a shift from T helper (Th)1 to Th2-dominating immunity in the peripheral system[15]. This alteration of immune responsiveness commences in

[1]Department of Molecular Microbiology and Immunology, University of Southern California, Keck School of Medical, Zilkha Neurogenetic Institute, 1501 San Pablo Street, Los Angeles, CA 90033, USA. [2]Division of Maternal-Fetal Medicine, Department of Obstetrics and Gynecology, University of Southern California, Keck School of Medicine, Zilkha Neurogenetic Institute, 1501 San Pablo Street, Los Angeles, CA 90033, USA. [3]Department of Microbiology, Immunology and Molecular Genetics, University of California, Los Angeles, CA 90095, USA. [4]Department of Cell and Neurobiology, University of Southern California, Keck School of Medicine, Zilkha Neurogenetic Institute, 1501 San Pablo Street, Los Angeles, CA 90033, USA. [5]Division of Pediatric Infectious Diseases, David Geffen School of Medicine, University of California, Los Angeles, Marion Davies Children's Health Center, 10833 LeConte Avenue, Los Angeles, CA 90095, USA. [6]Laboratório de Pesquisa Clínica em Doenças Febris Agudas, Instituto Nacional de Infectologia Evandro Chagas, FIOCRUZ, 4365 Avenida Brasil, Rio de Janeiro, RJ 21040-360, Brazil. *e-mail: jaeujung@med.usc.edu

early pregnancy when blood monocytes recruited to the placenta are converted into M2 macrophages to ensure an immunosuppressive environment for fetus development[10]. Activated monocytes are cytokine factories capable of secreting immune mediators that, in turn, further direct monocyte differentiation. For instance, C–X–C motif chemokine ligand (CXCL)10, interleukin (IL)-23A, IL-12, CD64, CD80, indoleamine 2,3-dioxygenase (IDO), suppressor of cytokine signalling 1 (SOCS1) and C–C chemokine receptor type 7 (CCR7) promote differentiation into M1 macrophages, whereas IL-10, arginase (Arg)-1, CD200R, CD163, CD23, C–C motif chemokine 22 (CCL22), vascular endothelial growth factor A (VEGFα), chitinase-3-like protein 1 (CHI3L1/YKL-40) and transforming growth factor beta prime M2 macrophage polarization[16–21]. Indeed, overt activation of monocytes and/or macrophages can induce excessive cytokine production, which leads to pregnancy complications, such as pre-elampsia[10,22].

Despite the established placental tropism of ZIKV, little is known about the target cells in the blood and their immune responses elicited by ZIKV viraemia. Here we identified CD14+ monocytes as the primary target for the infection of two different lineages of ZIKV, which ultimately promoted differential monocytic shifts. Asian ZIKV infection induced the pronounced expansion of non-classical monocytes that leads to the M2-skewed immunosuppressive phenotype as evidenced by the overt production of IL-10. In contrast, African ZIKV infection promoted inflammatory M1-skewed immune responses along with the specific induction of CXCL10 by intermediate monocytes. Furthermore, blood from pregnant women showed an enhanced infectivity to African and Asian ZIKV, which leads to pronounced M1/M2-skewed immune responses. Finally, a multiplex cytokine array of sera from ZIKV+ symptomatic pregnant women also showed increased levels of M2-skewed immunosuppressive cytokines and fibronectin-1 (FN1) associated with pregnancy complications. This study demonstrates the differential phenotypic responses of human blood monocytes induced by different lineages of ZIKV after infection and sheds important insights into the pronounced immune responses present during pregnancy.

Results

ZIKV specifically targets human CD14+ blood monocytes, inducing phenotypic shift. Infections of heparinized whole blood obtained from healthy donors were performed using African ZIKV (MR766) and Asian ZIKV (H/PF/2013) at multiplicity of infection (MOI) 1 (Fig. 1a). At 24 hour post-infection (hpi), peripheral blood mononuclear cells (PBMCs) were isolated from whole-blood specimens and the susceptibility to ZIKV infection was determined using viral-load quantitative real-time (qRT)-PCR and fluorescence-activated cell sorting (FACS). Interestingly, despite a 90% sequence identity between the ZIKV MR766 and H/PF/2013 strains, a significantly higher viral burden was detected in PBMCs infected with the MR766 strain than in those infected with the H/PF/2013 strain (Fig. 1b). To identify the primary target cells of ZIKV infection, we sorted and gated the isolated PBMCs by flow cytometry into four major blood immune subsets (monocytes, natural killer (NK) cells, T cells and B cells) (Supplementary Fig. 1a), followed by detection of the ZIKV NS1 RNA and envelope (E) protein. Viral load and FACS analyses identified CD14+ monocytes among these sorted immune subsets as the primary target cells for ZIKV infection (Fig. 1c,d). Similarly, higher viral burdens were detected in CD14+ monocytes infected with the MR766 strain than in those infected with the H/PF/2013 strain (Fig. 1c,d).

CD14hi CD16− classical monocytes are the dominant monocyte subsets in blood and rapidly undergo activation and phenotypic shift on stimulation. To determine whether ZIKV infections drive the phenotypic shift of classical monocytes into other subsets, we examined ZIKV-infected monocytes using CD14 and CD16 surface markers (Supplementary Fig. 1b). Indeed, either MR766 or

H/PF/2013 ZIKV infection induced a specific expansion of CD14lo CD16+ non-classical monocytes, but not that of CD14hi CD16+ intermediate monocytes. Surprisingly, despite its lower virus burden, H/PF/2013-infected monocytes showed a significantly higher expansion of CD14lo CD16+ non-classical monocytes than MR766-infected monocytes (Fig. 1e). These data identified CD14+ monocytes as the primary target cells for ZIKV infection, in which the H/PF/2013 strain drives a higher expansion of CD14lo CD16+ non-classical monocytes despite its lower viral burden when compared with the MR766 strain.

Different lineages of ZIKV differentially affect expressions of cytokines and immune modulatory genes. Activated monocytes are key producers of cytokines in blood, which subsequently influence the monocyte differentiation. To determine whether ZIKV infection affects cytokine expression, PBMCs were isolated from whole blood at 24 hpi with MR766 ZIKV or H/PF/2013 ZIKV and subjected to qRT-PCR screening for 43 cytokines and immune modulatory genes commonly associated with acute viral infection, which were further categorized into four different pathways (type I interferon (IFN)-related signalling, inflammation, M1-skewed pro-inflammation and M2-skewed immunosuppression). Heat-map representation revealed the contrasting induction pattern of cytokines and immune mediators in response to the infection with two different lineages of ZIKV strains (Fig. 2a). MR766-infected whole blood exhibited an apparent increase of IFN-β in plasma, whereas little or no increase of IFN-β was detected on H/PF/2013 infection (Fig. 2b). Consistently, MR766 infection elicited a significantly higher induction of the *signal transducer and activator of transcription (STAT)1/2, 2′,5′-oligoadenylate synthetase (OAS) 1/3, viperin, IFN regulatory factor 7/9 and nuclear factor kappa B (NF-κB)* subunits p50 p65 when compared with H/PF/2013 infection (Fig. 2c and Supplementary Fig. 2a). Interestingly, a panel of cytokines and immune modulatory genes (*CXCL10, IL-23A, CD64, CD80, IL-18, IDO, SOCS1* and *CCR7*) associated with M1-skewed inflammation was profoundly induced specifically on MR766 infection (Fig. 2d and Supplementary Fig. 2c). By striking contrast, H/PF/2013-infected PBMCs demonstrated a significant elevation of M2-skewed immunosuppression-related genes (*IL-10, Arg-1, CD200R, CD163, CD23, CCL22* and *VEGFα*) (Fig. 2e and Supplementary Fig. 2d).

As CXCL10 and IL-10 cytokines are crucial for priming monocytes and/or macrophages into pro-inflammatory M1-skewed and immunosuppressive M2-skewed phenotypes, respectively[17], we sorted mock- and ZIKV-infected PBMCs into monocytes, NK cells, T cells and B cells, followed by qRT-PCR analysis. These results showed the specific induction of *CXCL10* and *IL-10* expressions in ZIKV-infected CD14+ monocytes. Strikingly, MR766-infected monocytes exhibited a high level of *CXCL10* expression, whereas a high *IL-10* expression was detected in H/PF/2013-infected monocytes (Fig. 2f). Consistent with these observations, enzyme-linked immunosorbent assay (ELISA) performed on the plasma of mock- and ZIKV-infected whole-blood specimens at 24 hpi showed that a considerable production of CXCL10 was detected on MR766 infection, whereas a significant production of IL-10 was observed on H/PF/2013 infection (Fig. 2g). Together, these data indicate that the different lineages of ZIKV differentially affect the expression of cytokine and immune modulatory genes associated with M1- or M2-skewed monocytes and/or macrophage phenotypes.

Asian ZIKV preferentially targets non-classical monocytes, driving specific IL-10 expression. To address further the differential expansion of monocyte subsets on infection with different lineages of ZIKV, we infected total monocytes isolated from human whole blood with H/PF/2013 or MR766, followed by sorting into individual monocyte subsets (Fig. 3a). Despite infection at the same MOI, the H/PF/2013 strain showed much
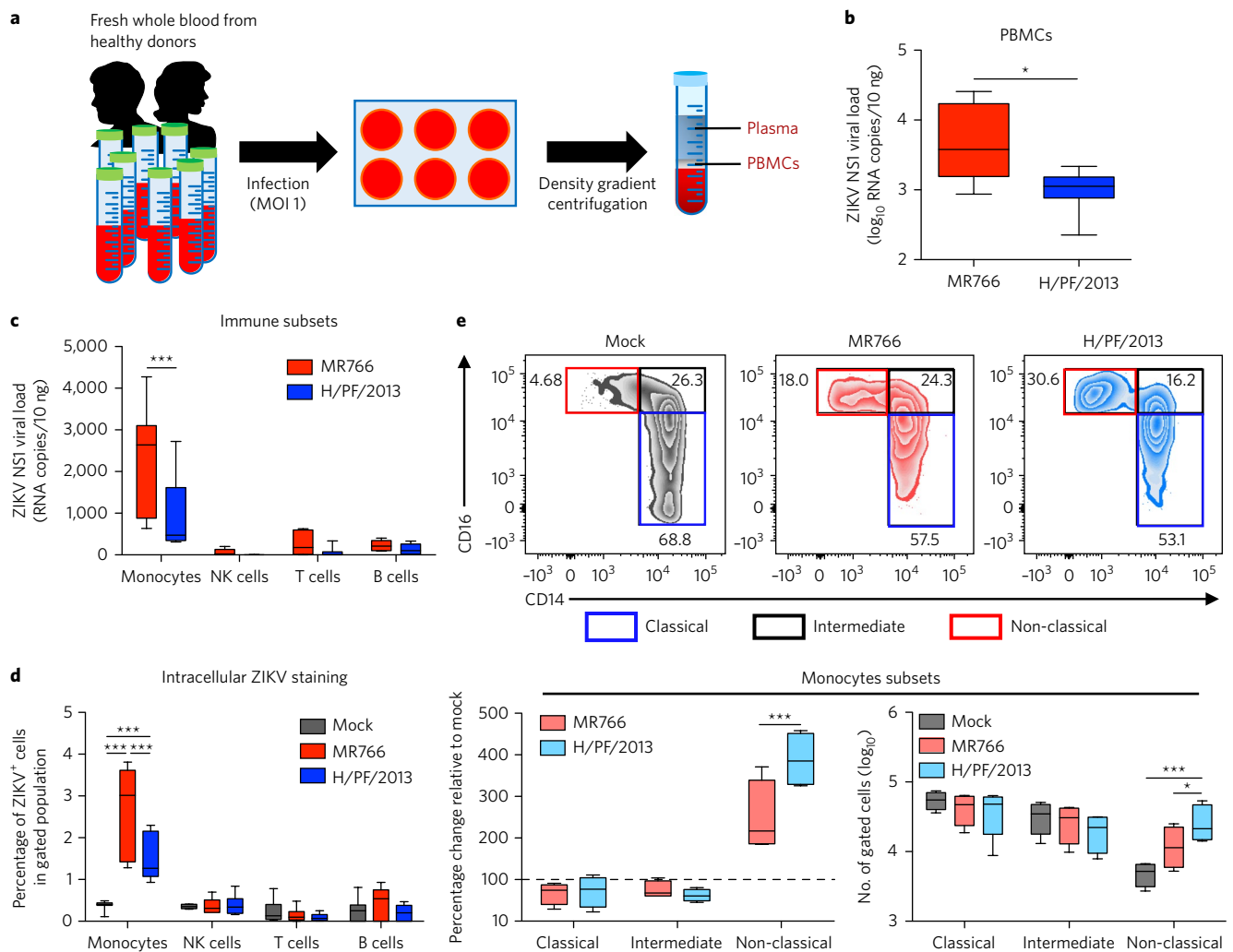
Fig. 1 | ZIKV infects CD14+ monocytes and drives the monocyte subset shift to the CD16+ non-classical subset during whole-blood infection. Whole blood derived from healthy donors ($n = 8$) was infected with African ZIKV (MR766) or Asian ZIKV (H/PF/2013) at MOI 1 for 24 h. PBMCs were isolated at 24 hpi for FACS or RNA extraction. **a**, Schematic representation of the experimental set-up. **b,c**, Viral burden of total PBMCs (**b**) and sorted immune subsets (CD45+ CD14+ monocytes, CD45+ CD56+ NK cells, CD45+ CD3+ T cells and CD45+ CD19+ B cells) (**c**) were detected using viral-load qRT-PCR with the specific probes and primers against the ZIKV NS1 RNA. **d**, Intracellular ZIKV Env antigens in various blood subsets were determined using FACS. **e**, Flow-cytometry profiling of classical (CD14hi CD16-), intermediate (CD14hi CD16+) and non-classical (CD14lo CD16+) monocyte subsets of mock- and ZIKV-infected PBMCs expressed as the percentage change relative to mock controls, or presented as the number of cells per subset within a gated CD45hi SSChi myeloid population (10^5 cells). Data (mean ± s.e.m.) are presented in box plots showing the upper (75%) and lower (25%) quartiles, with the horizontal line as the median and the whiskers as the maximum and minimum values observed. $*P < 0.05$, $***P < 0.001$, Mann–Whitney U test in **b** and two-way ANOVA, Bonferroni post-test in **c–e**.

lower viral loads in infected monocytes than the MR766 strain (Fig. 3b,d). As -differentiation of monocytes to macrophages takes 3–5 days post-stimulation[23,24], mock- or ZIKV-infected monocytes were harvested at 2 days post-infection (dpi) for the apparent detection of M1- and/or M2-skewed markers, and subsequently sorted into individual monocyte subsets. This showed that H/PF/2013 infection led to the apparent decrease of classical monocytes in conjunction with the considerable increase of non-classical monocytes (Fig. 3c). Analysis of the ZIKV intracellular E protein and NS1 RNA load revealed that MR766 preferentially infects intermediate monocytes, whereas H/PF/2013 infects non-classical monocytes at a higher magnitude (Fig. 3e,f). Furthermore, MR766-infected classical/intermediate monocytes exhibited a high level of *CXCL10* expression, whereas a high *IL-10* expression was detected in H/PF/2013-infected non-classical monocytes (Fig. 3g,h). Finally, infection with either MR766 or H/PF/2013 did not elicit detectable cell death at 48 hpi (Fig. 3i).

These data further demonstrate that different lineages of ZIKV infection differentially target M1- or M2-skewed monocyte subsets.

Different immunologic traits between African- and Asian-lineage ZIKV strains. To test that differential levels of virus infectivity, non-classical monocyte expansion and immunoregulatory gene expression were a conserved immunologic trait between African- and Asian-lineage ZIKV strains, samples of whole human blood were infected with additional African-lineage IbH30656 and Asian-lineage PRVABC59 ZIKV strains at different MOIs, and PBMCs and plasma were isolated at 40 hpi. Consistent with previous results (Fig. 1b), a lower ZIKV burden was observed on infection with Asian ZIKV PRVABC59 and H/PF/2013 when compared with infection with the African ZIKV counterparts MR766 and IbH30656 (Supplementary Fig. 3a,d). Furthermore, the apparent expansions of CD14lo CD16+ non-classical monocytes was observed after ZIKV PRVABC59 infection, whereas a minimal
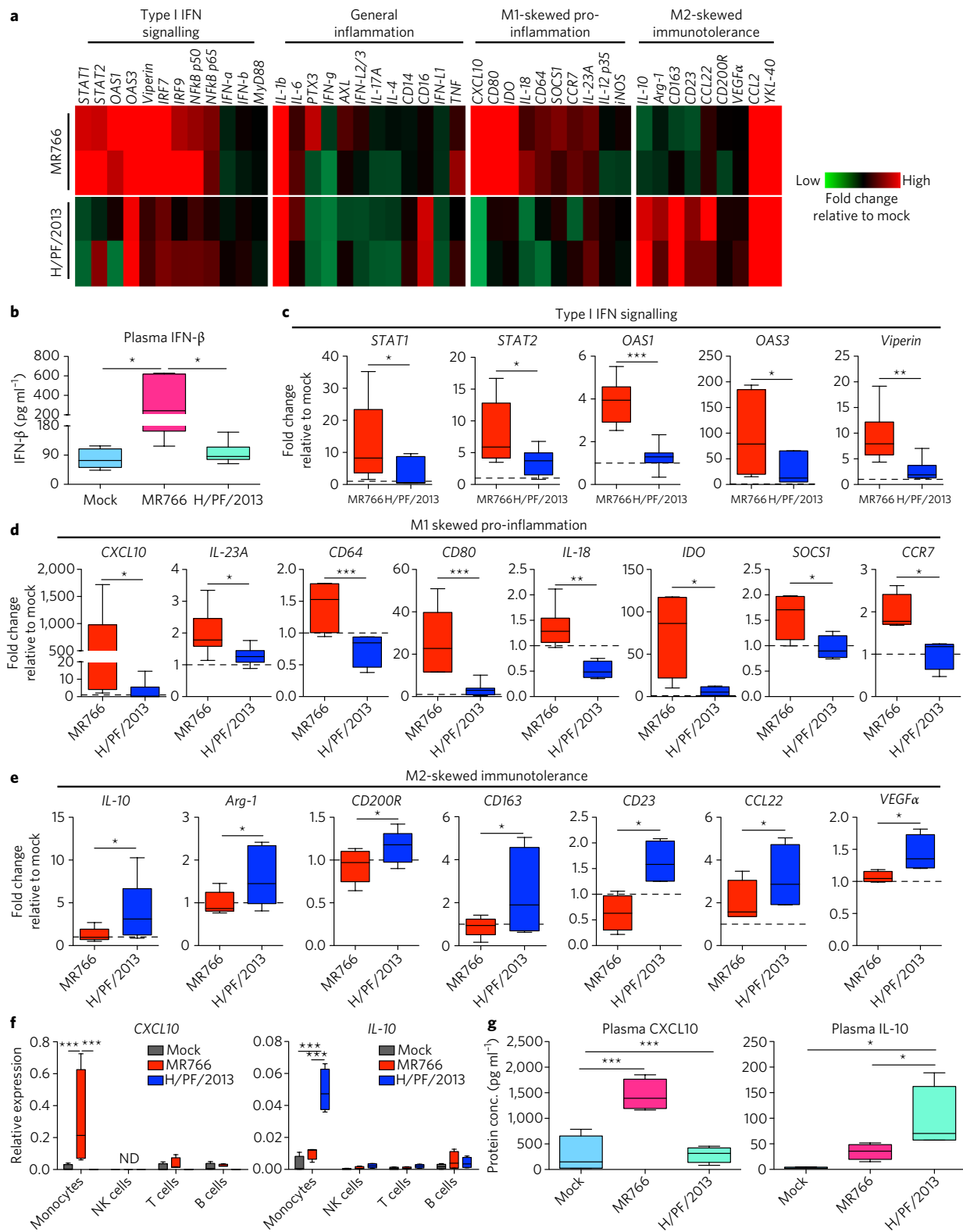
Fig. 2 | Different lineages of ZIKV infection of whole blood elicit differential immunomodulatory responses. Mock- or ZIKV-infected PBMCs and plasma were isolated from the whole blood of an equal number of male and female donors ($n = 8$) at 24 hpi. **a**, Representative heat map of 43 immune mediator profiles in PBMCs. **b**, The plasma IFN-β level was determined by ELISA. **c**–**e**, Gene-expression profiles of type I IFN signalling genes (*STAT1/2*, *OAS1/3* and *viperin*) (**c**), M1-skewed pro-inflammatory genes (*CXCL10*, *IL-23A*, *CD64*, *CD80*, *IL-18*, *IDO*, *SOCS1* and *CCR7*) (**d**) and M2-skewed immunosuppression genes (*IL-10*, *Arg-1*, *CD200R*, *CD163*, *CD23*, *CCL22* and *VEGF*) (**e**) were normalized to *GAPDH* and expressed as fold changes relative to mock controls. **f**, CXCL10 and IL-10 protein expressions within isolated plasma specimens ($n = 8$) were determined using ELISA. **g**, *CXCL10* and *IL-10* mRNA expressions within sorted immune subsets from isolated PBMCs ($n = 4$) using qRT-PCR. Data (mean ± s.e.m.) are presented in box plots showing the upper (75%) and lower (25%) quartiles, with the horizontal line as the median and the whiskers as the maximum and minimum values observed. *$P < 0.05$, **$P < 0.01$, ***$P < 0.001$, Mann–Whitney U test in **c**–**e**, one-way ANOVA for **b** and **f** and two-way ANOVA, Bonferroni post-test in **g**. Conc., concentration.
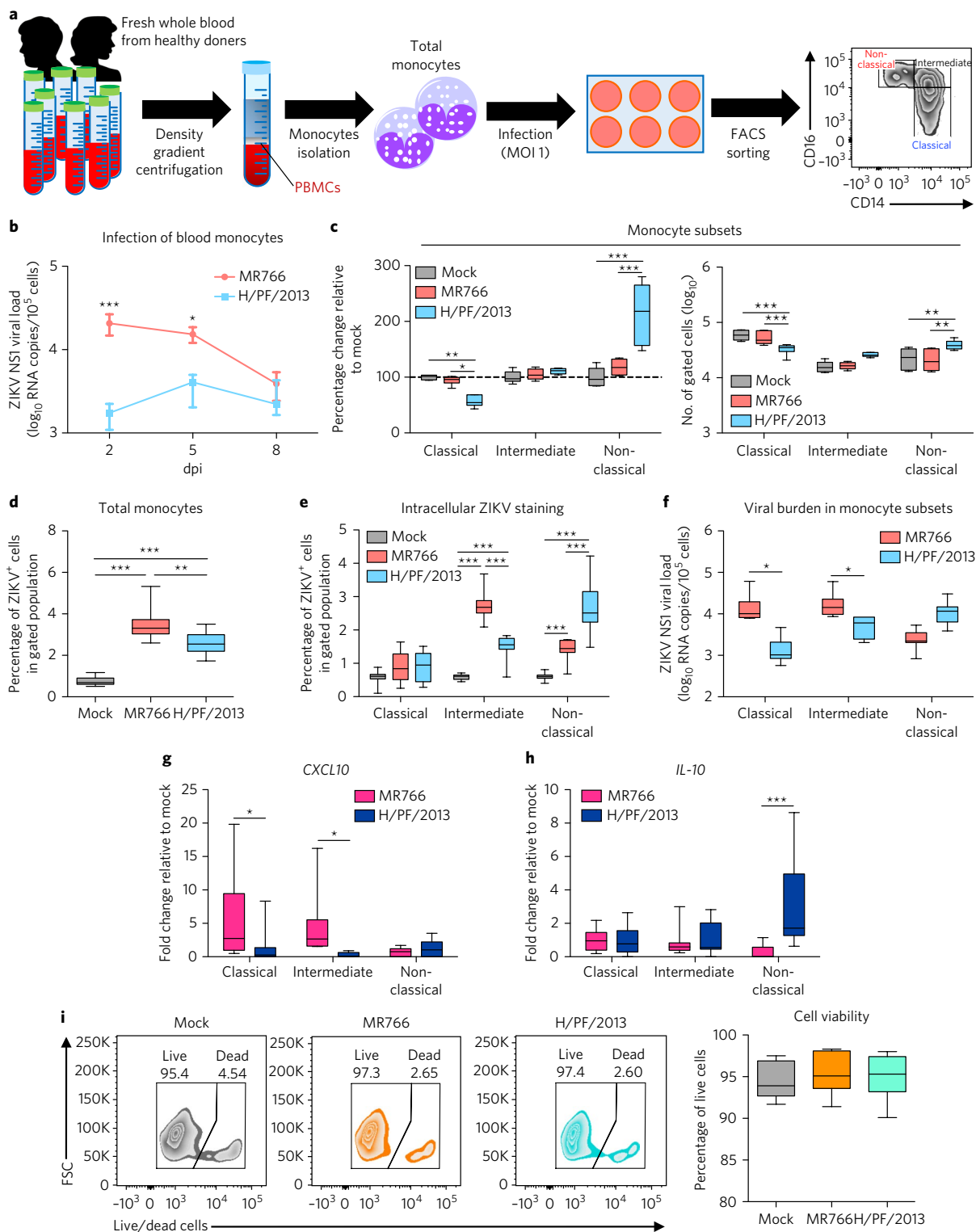
Fig. 3 | Asian ZIKV preferentially targets non-classical monocytes, driving specific *IL-10* expression. PBMCs were isolated from the whole blood derived from healthy donors ($n=6$–11), followed by African ZIKV (MR766) or Asian ZIKV (H/PF/2013) infections at MOI 1 for 2, 5 or 8 dpi. **a**, Schematic representation of the experimental set-up. **b**, Viral burden of total monocytes ($n=6$) during longitudinal infections detected using viral-load qRT-PCR with the specific probes and primers against the ZIKV NS1 RNA. **c**, Flow-cytometry profiling of classical (CD14^{hi} CD16$^-$), intermediate (CD14^{hi} CD16$^+$) and non-classical (CD14^{lo} CD16$^+$) monocyte subsets of mock- and ZIKV-infected monocytes expressed as the percentage change relative to mock controls, or presented as the number of cells per subset within a gated CD45^{hi} SSC^{hi} myeloid population (10^5 cells). **d,e**, At 2 dpi, the total monocytes ($n=11$) were harvested to determine the infectivity of the total monocytes (**d**) or gated monocyte subsets using intracellular ZIKV Env antigen staining by FACS (**e**). **f**, Viral burdens were determined within sorted monocyte subsets using viral-load qRT-PCR. **g,h**, CXCL10 (**g**) and IL-10 (**h**) mRNA expressions within sorted monocyte subsets were determined using qRT-PCR. **i**, Cell viabilities of the total monocytes were determined using live/dead staining by FACS analysis. Data (mean±s.e.m.) are presented in box plots showing the upper (75%) and lower (25%) quartiles, with the horizontal line as the median and the whiskers as the maximum and minimum values observed. *$P<0.05$, **$P<0.01$, ***$P<0.001$, two-way ANOVA in **b**, **c**, **e**–**h** or one-way ANOVA, Bonferroni post-test in **d** and **i**.

increase of CD14^{lo} CD16$^+$ non-classical monocytes was observed after African ZIKV IbH30656 infection (Supplementary Fig. 3b,e). Similarly, the robust induction of *CXCL10* expression was observed on African ZIKV IbH30656 infection, but not on ZIKV PRVABC59 infection. In contrast, *IL-10* expression was induced only on Asian ZIKV PRVABC59 infection (Supplementary Fig. 3c,f). Thus, these results demonstrate that a lower virus burden, non-classical monocyte expansion and M2-skewed immunosuppression gene expression are commonly associated with Asian ZIKV strains, whereas a higher virus burden and M1-skewed inflammatory gene expression are triggered by African ZIKV strains.

Pregnancy is associated with enhanced ZIKV infection and profound monocyte subset shift. Despite numerous clinical cohort studies of ZIKV-infected pregnant women, the exact acute immunological effects induced by ZIKV infection remain unknown. To investigate if ZIKV differentially altered blood immunity during different trimesters of pregnancy, we infected whole -blood specimens obtained from women in their first, second and third trimester of gestation. Whole-blood specimens of age-matched non-pregnant women were included as controls. Higher viral burdens were detected in PBMCs isolated from first trimester pregnant women after ZIKV MR766 and H/PF/2013 infections, as compared with non-pregnant women, albeit higher viral loads were detected after MR766 infection than after H/PF/2013 infection (Fig. 4a,b). We further confirmed that CD14$^+$ monocytes were the primary target cells for ZIKV infection during pregnancy, and that the H/PF/2013 strain showed a lower viral infection in these monocytes than that of the MR766 strain (Fig. 4c). Surprisingly, H/PF/2013 infection induced a dramatic expansion of CD14^{lo} CD16$^+$ non-classical monocytes in maternal blood from the first and second trimesters of pregnancy, whereas blood from the third trimester of pregnancy exhibited a non-classical monocyte expansion similar to blood from non-pregnant women (Fig. 4d,e). Compared with H/PF/2013 infection, a small increase of non-classical monocytes was observed with MR766 infection of blood from non-pregnant and pregnant women in all the trimesters of pregnancy (Fig. 4d,e). These results provide the first experimental evidence that the early stage of pregnancy is a period of high susceptibility to ZIKV infection, which leads to a dramatic expansion of CD14^{lo} CD16$^+$ non-classical monocytes in maternal blood.

Differential expression of immune modulatory genes in the blood of pregnant women on African- or Asian-lineage ZIKV infection. Next, we characterized the expression profiles of IFN-signalling related genes, M1-skewed inflammation genes and M2-skewed immunosuppression genes in PBMCs isolated from the blood of pregnant and non-pregnant women at 40 hpi with ZIKV (Fig. 5a). MR766 infection induced IFN-β production in the plasma of pregnant and non-pregnant women, albeit a significantly lower level of IFN-β production was noted in the plasma of pregnant women as compared with that of non-pregnant women (Fig. 5a). On the other hand, H/PF/2013 infection led to a lower IFN-β response in the blood of both pregnant and non-pregnant women than MR766 infection (Figs. 2b and 5a). In addition, *STAT1/2*, *OAS1/3* and *viperin* expressions in the blood of pregnant women were highly elevated after MR766 infection, but not after infection with H/PF/2013 (Fig. 5b).

Pregnancy intrinsically displays a high magnitude of M2-polarized gene expression, particularly during the first and second trimesters[11]. For the mock-infection condition, the expression of M2-skewed immunosuppression markers (*IL-10*, *Arg-1*, *CD200R*, *YKL-40*, *CD163* and *VEGFα*) was significantly higher in the blood of pregnant women than in that of non-pregnant subjects (Supplementary Fig. 4a). In contrast, the suppression of *CXCL10* and *IL-23A* expressions was observed in blood from pregnant subjects,

whereas the expression of other M1-related markers was unchanged regardless of pregnancy status (Supplementary Fig. 4b). On MR766 infection, plasma CXCL10 levels were elevated significantly in the plasma of both non-pregnant and pregnant subjects, though to a lesser extent in that of pregnant women (Fig. 5c). Similarly, the expression of M1-skewed inflammation related genes, including *CXCL10*, *IDO*, *CD80*, *CCR7*, *SOCS1*, *IL-23A*, *IL-12 p35* and *IL-18*, was highly induced in MR766-infected blood from pregnant women (Fig. 5d and Supplementary Fig. 4c). Despite elevated basal plasma IL-10 levels and the expression of M2-related genes during pregnancy (Fig. 5e and Supplementary Fig. 4a), H/PF/2013 infection further enhanced plasma IL-10 levels in the plasma of pregnant women, particularly during the first and second trimesters (Fig. 5e), and the *CCL22* and *YKL-40* expression in their blood (Fig. 5f). In addition, the expression of M2-related genes (*IL-10*, *Arg-1*, *CD200R*, *CCL22*, *YKL-40* and *CCL2*) in the blood of non-pregnant women was also increased on H/PF/2013 infection, but not after MR766 infection (Fig. 5f and Supplementary Fig. 4d). Finally, multiplex cytokine array analyses of sera from 30 RT-PCR confirmed ZIKV$^+$ symptomatic pregnant women and 14 healthy control pregnant women demonstrated overt expression of M2-skewed immunosuppressive cytokines IL-10, CD163 and YKL-40, but not that of M1 cytokine IL-12 p40, in sera of ZIKV$^+$-infected pregnant women (Fig. 5g–j). Serum IL-10 was elevated, particularly in the first and second trimesters of pregnancy, in ZIKV$^+$ women, whereas serum CD163 and YKL-40 were significantly increased in all trimesters of pregnancy in ZIKV$^+$ women (Fig. 5g–i). Finally, serum IL-10, CD163 and YKL-40 were considerably high in ZIKV$^+$-viraemic or viruric pregnant women than in healthy control pregnant women (Fig. 5g–i). Together, analyses of in vitro infection and that of patient specimens clearly demonstrate that Asian ZIKV infection preferentially leads to the M2-skewed immunosuppression phenotype host immune response.

Transcriptome analysis of blood monocytes on MR766 or H/PF/2013 ZIKV infection. As CD14$^+$ monocytes were the primary target cells for ZIKV infection in blood, we isolated total monocytes from mock- and ZIKV-infected whole blood at 40 hpi, followed by a multiplexed gene-expression analysis using the NanoString nCounter platform that targets ~600 myeloid cell-related genes (Supplementary dataset 1). Analysis of the infected non-pregnant women's monocytes revealed the specific induction of a larger pool of myeloid cell-related genes on infection with MR766 (75 genes) than with H/PF/2013 (42 genes) (Fig. 6a and Supplementary Fig. 4a). In addition, MR766 infection led to a higher induction of IFN-signalling pathway genes compared with H/PF/2013 infection (Supplementary Fig. 4b). Most host genes induced by MR766 infection were M1-skewed inflammation-related (*CXCL10*, *IL-12B* and *prostaglandin-endoperoxide synthase 2* (*PTGS2*)) and pro-inflammatory genes (*complement factor 3* (*C3*), *resistin-like beta* (*RETNLB*), *ribonuclease A family member 3* (*RNASE3*) and *IL-27*), whereas H/PF/2013-infection-induced host genes were M2-skewed immunosuppression related (*IL-10*, *IL-4* and *platelet-derived growth factor subunit B* (*PDGFB*)) (Fig. 6b). In addition, H/PF/2013 infection induced host genes for fatty acid oxidation (*lipoprotein lipase* (*LPL*)) and collagen deposition (*ADAMTS14*, *discoidin domain-containing receptor 2* (*DDR2*) and *collagen alpha-1(X) chain* (*COL10A1*)) that are crucial for M2 macrophage function (Fig. 6b). Interestingly, unlike monocytes from non-pregnant women, which showed the unique induction of a larger pool of myeloid cell-related genes after MR766 infection rather than H/PF/2013 infection (Fig. 6a and Supplementary Fig. 4a), monocytes from pregnant women were more reactive to H/PF/2013 infection than to MR766 infection (Fig. 6c). Consistent with a clinical study showing that Asian ZIKV infection during the first and second trimester led to a significantly higher frequency of fetal anomalies[25,26],
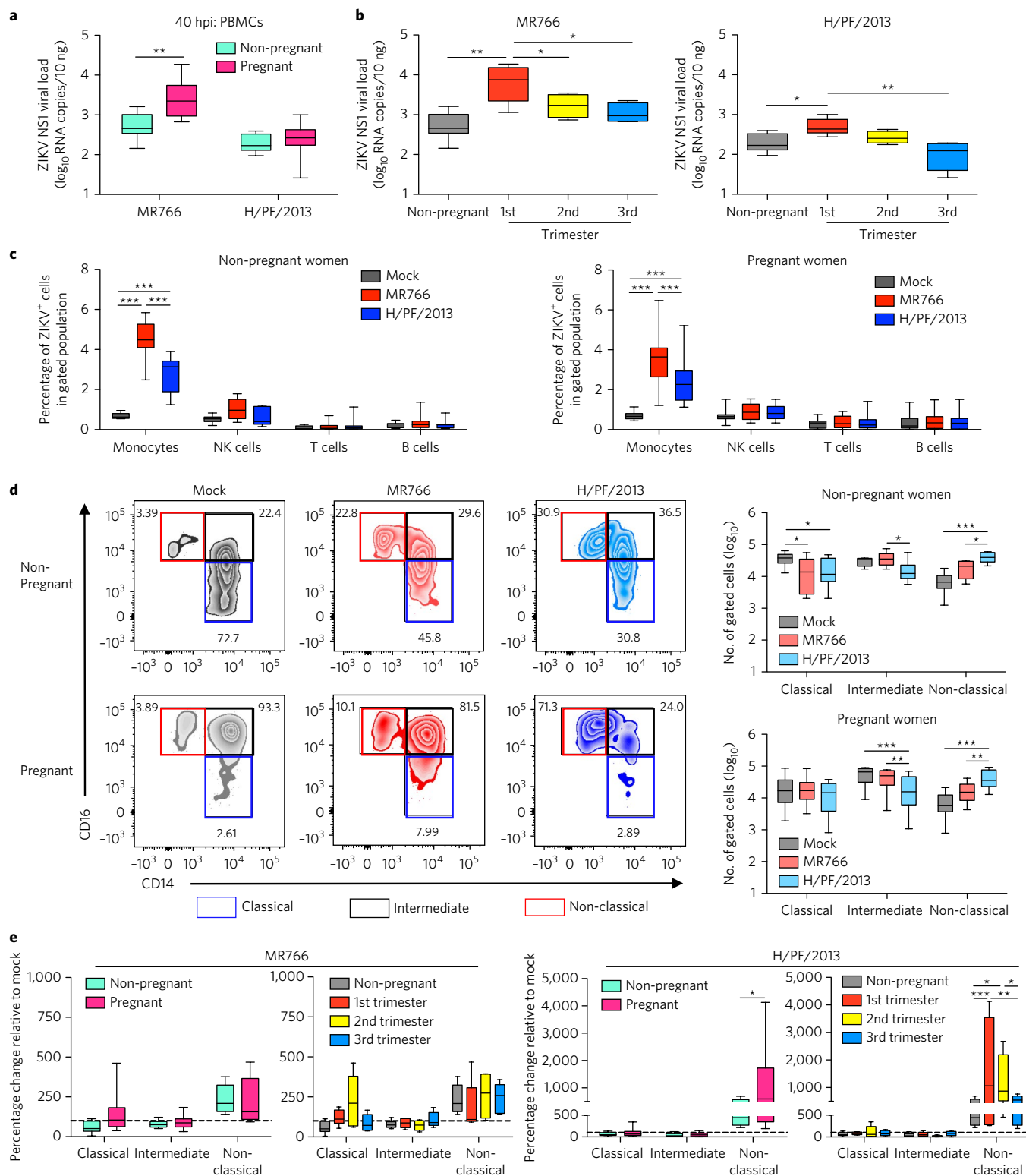
Fig. 4 | Pregnancy is associated with enhanced ZIKV infection and a profound monocyte-subset shift. Whole blood was obtained from healthy non-pregnant ($n = 10$) and pregnant women ($n = 5$ per trimester) who were in the first (1st), second (2nd) or third (3rd) trimester of pregnancy. ZIKV infections were performed at MOI 1 and PBMCs were isolated at 40 hpi. **a,b**, Viral burdens within the total PBMCs of non-pregnant and pregnant subjects (**a**) or non-pregnant and pregnant women in each trimester (**b**) were detected using viral-load qRT-PCR with the specific probes and primers against the ZIKV NS1 RNA. **c**, Intracellular ZIKV E antigen in various blood subsets (CD45$^+$ CD14$^+$ monocytes, CD45$^+$ CD56$^+$ NK cells, CD45$^+$ CD3$^+$ T cells and CD45$^+$ CD19$^+$ B cells) were determined using FACS. **d,e**, Flow-cytometry profiling of classical (CD14^{hi} CD16$^-$), intermediate (CD14^{hi} CD16$^+$) and non-classical (CD14^{lo} CD16$^+$) monocyte subsets present within mock- and ZIKV-infected PBMCs presented as the number of cells per subset within a gated CD45^{hi} SSC^{hi} myeloid population (10^5 cells) (**d**) or expressed as the percentage change relative to mock controls (**e**). Data (mean ± s.e.m.) are presented in box plots showing the upper (75%) and lower (25%) quartiles, with the horizontal line as the median and the whiskers as the maximum and minimum values observed. *$P < 0.05$, **$P < 0.01$, ***$P < 0.001$, two-way ANOVA, Bonferroni post-test in **a** and **c**–**e** or one-way ANOVA, Bonferroni post-test in **b**.
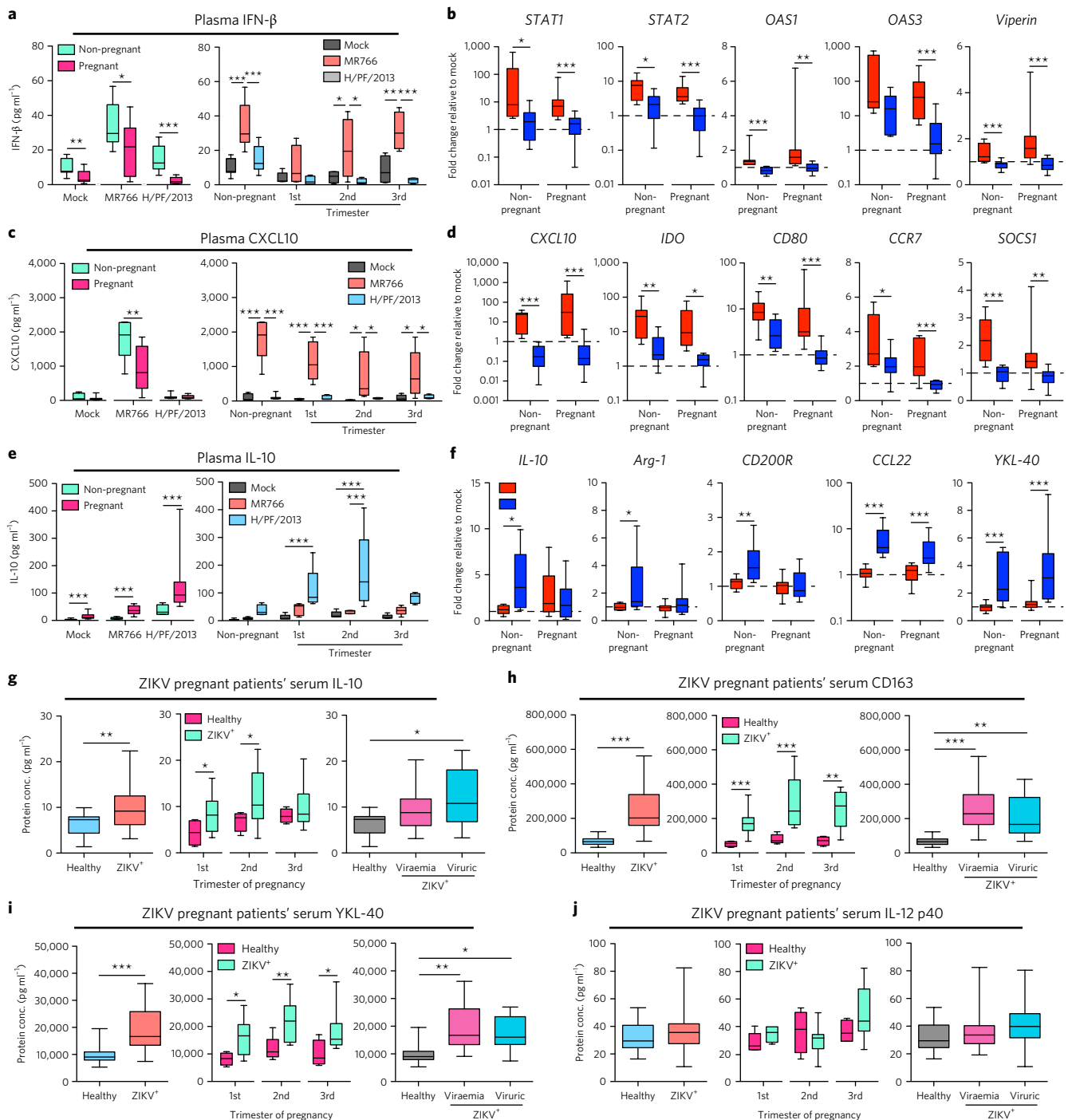
Fig. 5 | Pregnancy exacerbates Asian-ZIKV-induced M2-skewed immunosuppression. Mock- or ZIKV-infected PBMCs (MOI 1) and plasma were isolated from the whole blood of non-pregnant ($n=10$) and pregnant women ($n=5$ per trimester) at 40 hpi. **a–f**, Protein expressions of IFN-β (**a**), CXCL10 (**c**) and IL-10 (**e**) within plasma isolated from mock- or ZIKV-infected whole blood were determined using ELISA; gene-expression profiles of IFN-related genes (*STAT1/2*, *OAS1/3* and *viperin*) (**b**), M1 macrophage-related genes (*CXCL10*, *IDO*, *CD80*, *CCR7* and *SOCS1*) (**d**) and M2 macrophage-related genes (*IL-10*, *Arg-1*, *CD200R*, *CCL22* and *YKL-40*) (**f**) were normalized to *GAPDH* and expressed as fold change relative to mock controls. **g–j**, Multiplex cytokine analyses of IL-10 (**g**), sCD163 (**h**), YKL-40 (**i**) and IL-12 p40 (**j**) of serum specimens derived from healthy pregnant women ($n=4$–5 per trimester) and ZIKV$^+$ pregnant women ($n=10$ per trimester). Data (mean ± s.e.m.) are presented in box plots showing the upper (75%) and lower (25%) quartiles, with the horizontal line as the median and the whiskers as the maximum and minimum values observed. $*P<0.05$, $**P<0.01$, $***P<0.001$, two-way ANOVA, Bonferroni post-test in **a**, **c** and **e** (right panel), Mann–Whitney U test in **a**, **c** and **e** (left panel), **b**, **d**, **f** and **g–j** (first two panels on the left) and one-way ANOVA, Bonferroni post-test in **g–j** (right panel).

H/PF/2013 infection induced the expression of a higher number of host genes in monocytes from women in their first and second trimesters of pregnancy than from women in their third trimester

of gestation or who were non-pregnant (Fig. 6c). Interestingly, we also observed that two host pregnancy-complication-associated genes ADAMTS9 and FN1 (refs [27–31]) were induced in PBMCs and
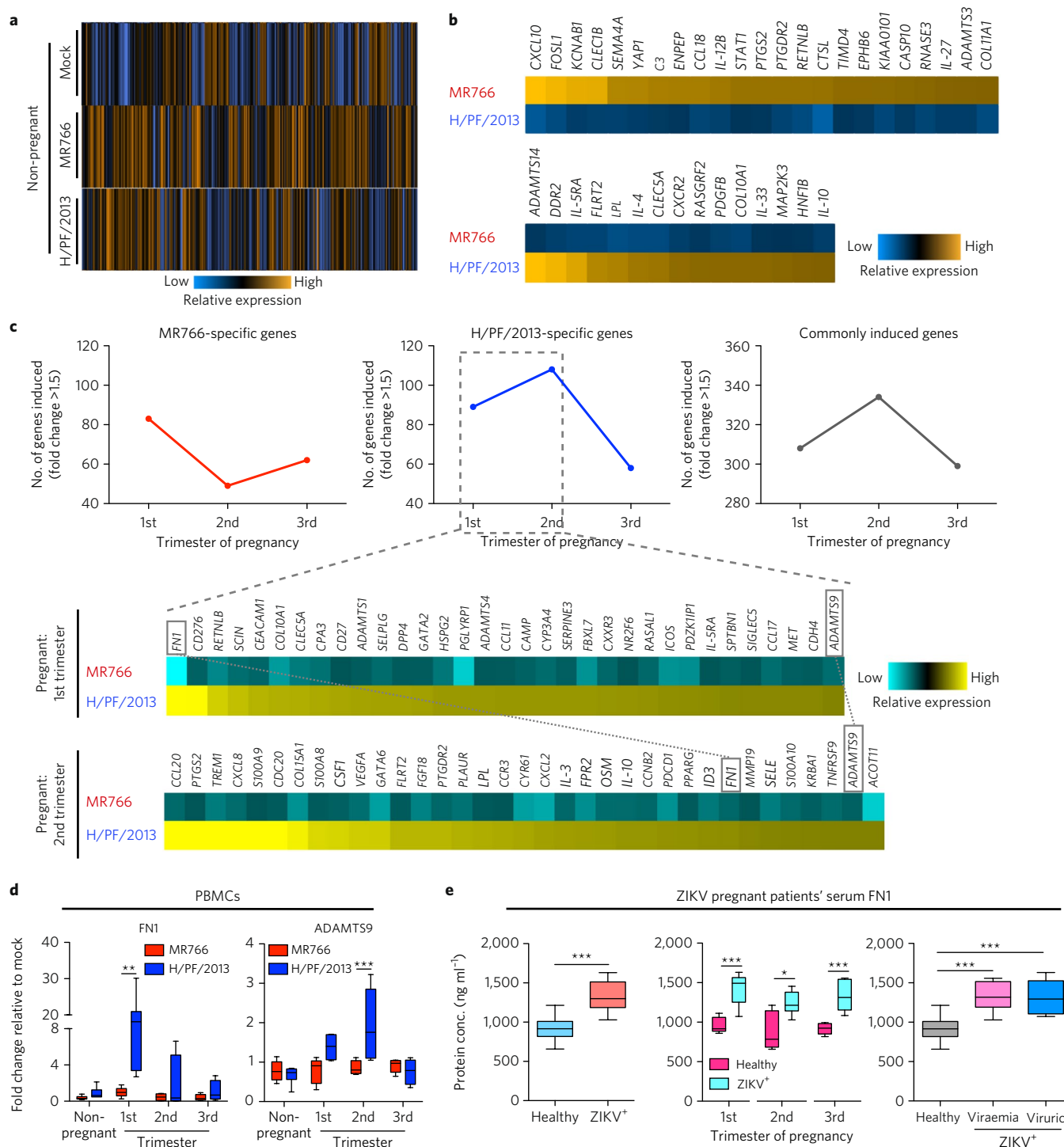
Fig. 6 | Transcriptome analysis of blood monocytes following African or Asian ZIKV infection. Pan monocytes including classical (CD14^{hi} CD16^{-}), intermediate (CD14^{hi} CD16^{+}) and non-classical (CD14^{lo} CD16^{+}) monocyte subsets were isolated from mock- and ZIKV-infected (MOI 1) PBMCs harvested at 40 hpi. Whole cell lysates of ~10,000 cells per specimen were subjected to NanoString multiplex gene analysis using the Human Myeloid panel that consists of ~600 genes. **a**, Venn diagram representation of the numbers of differentially induced genes between MR766 (African ZIKV) and H/PF/2013 (Asian ZIKV) of non-pregnant women specimens. **b**, Myeloid-related genes uniquely induced (fold change > 1.5) by MR766 or H/PF/2013 expressed as fold changes relative to mock controls and presented as heat maps. **c**, Myeloid-related genes uniquely induced by H/PF/2013 in 1st and 2nd trimester pregnant women are compared and presented as heat maps. *FN1* and *ADAMTS9* are highlighted to indicate the expression in both trimesters. **d**, Expression of the developmental genes *ADAMTS 9* and *FN1* in PBMCs (n = 10 for non-pregnant women; n = 5 per trimester for pregnant women) were normalized to *GAPDH* and expressed as fold changes relative to mock controls. **e**, ELISA analysis of FN1 in serum specimens derived from healthy pregnant women (n = 5 per trimester) and ZIKV^{+} pregnant women (n = 8–9 per trimester). Data (mean ± s.e.m.) are presented in box plots showing the upper (75%) and lower (25%) quartiles, with the horizontal line as the median and the whiskers as the maximum and minimum values observed. *P < 0.05, **P < 0.01, ***P < 0.001, two-way ANOVA, Bonferroni post-test in (**d**), Mann–Whitney U test in **e** (first two panels on the left) and one-way ANOVA, Bonferroni post-test in **e** (right panel).

monocytes of women in their first and second trimesters of pregnancy after Asian ZIKV infection (Fig. 6c,d). Indeed, serum FN1 exhibited significantly elevated levels in ZIKV+ pregnant patients in any trimester of pregnancy as well as in ZIKV+-viraemic or -viruric pregnant women (Fig. 6e). In summary, we demonstrate that infections with different lineages of ZIKV lead to different expression profiles of host immune genes and that this effect is dependent on pregnancy stage, especially during the first and second trimesters of gestation. Furthermore, our results show that Asian ZIKV infection induces the aberrant expression of host pregnancy-complication-associated genes *FN1* and *ADAMTS9*, which may contribute to adverse pregnancy outcomes.

Discussion

The recent re-emergence of ZIKV infection and its ominous association with congenital anomalies during pregnancy has captivated global attention[25,26,32,33]. Despite large clinical cohort studies of ZIKV-infected pregnant women, the dynamics of viral replication and blood immunity of ZIKV remains elusive. ZIKV viraemia in infected patients typically resolves in the first week of infection, as early as 72 hpi[34]. Owing to the short viraemic phase and mild clinical symptoms, to identify acute ZIKV patients and obtain their blood specimens has been a challenging task. So far, ZIKV replication dynamics has been largely studied using in vitro cell lines or in vivo IFN-α/β receptor knockout mouse model[35]; however, none of these systems may fully recapitulate human-blood infection. Specifically, the host target cells of ZIKV infection and the acute immune responses of blood after an infectious mosquito bite have not been well-studied. Hence, to overcome this issue, we utilized an in vitro human whole-blood infection approach that mimics the natural infection setting of ZIKV viraemia in humans. This approach has been shown to be an effective platform to dissect acute host immunity mediated against viruses, such as the Chikungunya virus and vaccinia virus[36,37]. Although the whole-blood infection approach has been a useful in vitro model for studying blood immunity, the caveat of this approach is the inability to access the infectivity of the non-PBMCs population, such as short-lived granulocytes. Here, we identified CD14+ monocytes as the primary target cells of acute ZIKV infection. Furthermore, higher viral burdens were detected in CD14+ monocytes infected with the African-lineage ZIKV strain than in those infected with the Asian-lineage ZIKV strain. The mechanisms responsible for this difference of replication kinetics between African-lineage ZIKV and Asian-lineage ZIKV in human CD14+ monocytes are under investigation.

Blood monocytes have been shown to be a favourable cellular target for several other viruses, such as the influenza A virus, vesicular stomatitis virus and vaccinia virus, and viral infections rapidly trigger differentiation of monocytes into dendritic cells[38]. Recently, Asian ZIKV infection of non-human primates was shown to trigger a peak of CD16+ monocyte activation at 2 dpi[39]. Here we showed that in human blood both lineages of ZIKV strains triggered the specific expansion of CD14lo CD16+ non-classical monocytes, but not the CD14hi CD16+ intermediate monocyte population. Although African-lineage ZIKV promoted a modest expansion of non-classical monocytes, it targeted intermediate monocytes as the preferred monocyte subset that specifically induced CXCL10-associated M1-skewed inflammatory responses. Surprisingly, despite a lower viral burden and infectivity, Asian-lineage ZIKV infection led to the large expansion of non-classical monocytes, the suppression of the type I IFN-signalling pathway and the promotion of the IL-10-associated M2-skewed immunosuppressive phenotype. Similar to other mosquito-borne RNA viruses, this immunophenotype was probably caused by a bystander effect. Previous studies have demonstrated that the infection of a small subset of blood cells with the Chikungunya virus is sufficient to trigger the robust activation of monocytes, which leads to a cytokine storm[37,40].

In addition, previous studies of HIV-1 infection-elicited immunodeficiency have suggested the possible pathogenic involvement of CD16+ monocytes through differentiation into M2 macrophages[41]. An expanded population of CD16+ monocytes has been specifically observed in human immunodeficiency virus (HIV) patients who experienced high viraemia, whereas patients who maintained undetectable viraemia showed reduced CD14lo CD16+ non-classical monocyte populations[42,43]. Just as the poor prognosis of HIV infection is closely associated with uncontrolled viraemia, the high viraemia of ZIKV has also been associated with lethality in patients with pre-existing medical conditions[44]. The unexpected resemblance of monocyte expansion and responses elicited by Asian ZIKV or HIV infection suggests that Asian ZIKV may trigger a certain degree of immunosuppression, whereby an inadvertent exacerbated disease outcome may occur in patients with underlying immune-altering conditions.

Pregnancy is a sophisticated biological process that relies on maternal-initiated immunosuppression towards the growing fetus, particularly during early to mid-stages of pregnancy, to ensure a healthy birth. A recent clinical study on 131 pregnant ZIKV+ patients has demonstrated that maternal viral burden and disease severity are not underlying risk factors for the development of fetal abnormalities[45]. However, prolonged ZIKV viraemia during the first trimester of pregnancy has been associated with fetal abnormalities[46,47], which suggests that the pregnancy stage of ZIKV infection may be risk determinant for ZIKV-associated birth defects. Interestingly, the infection of blood obtained from pregnant women, particularly those who were in their first trimester of pregnancy, exhibited enhanced viraemia after African or Asian ZIKV infection. This suggests that a higher viral burden would require a longer time to be cleared from the peripheral system, which leads to a prolonged viraemic phase. As monocytes from pregnant women did not show an obvious increase in infectivity, a slightly reduced IFN-β level during pregnancy may contribute to an enhanced viral burden. Indeed, ZIKV has been widely known to be highly sensitive to type I IFN signalling pathways[48,49]. In addition, it has been shown that pregnancy alone can induce the expansion of intermediate/non-classical monocytes with a declined classical subset[50]. Intriguingly, Asian ZIKV infection triggered pronounced changes in blood immunity specifically during the first and second trimester of pregnancy, which further promoted the dramatic expansion of CD14lo CD16+ non-classical monocytes and the apparent production of the IL-10 cytokine. The early-to-mid stages of healthy pregnancies occur in a Th2-bias environment in which IL-10 expression modestly increases to elicit a subtle immunosuppressive effect. However, the abundant production of IL-10 in response to Asian ZIKV is likely to do more harm than good with regards to the pregnancy outcome, as many viruses have been shown to exploit the elevated levels of IL-10 as a means to promote viral persistency and to dampen host defences[51–53]. Increased IL-10 levels have been detected in the amniotic fluid of pregnant ZIKV patients who had microcephalic fetuses or in neonates[54]. The highest frequencies of reported ZIKV-induced fetal defects were observed when the ZIKV infection occurred in the first and second trimesters of pregnancy[25,26]. Hence, we hypothesize that the expression of certain genes potentially detrimental to pregnancy may be induced in the first and second trimester specifically after Asian ZIKV infection. Indeed, the comparison of host genes uniquely induced by Asian ZIKV in monocytes from women in the first and second trimesters revealed high expressions of two pregnancy-detrimental genes—*ADAMTS9* and *FN1*. ADAMTS9 plays a crucial role in vascular remodelling during pregnancy[27]. Elevated *ADAMTS9* expression has been implicated in placental abnormalities, which leads to pre-term, small birth weight and/or labour arrest disorders[28,29]. Increased levels of *FN1* are found in pregnant women suffering from pregnancy complications, such as pre-eclampsia and fetal-growth restriction[30,31]. Surprisingly, we also

found that ZIKV⁺-viraemic or -viruric pregnant women showed elevated serum FN1 levels throughout all trimesters of pregnancy (Fig. 6e). Hence, our findings suggest the potential pathogenic roles of pregnancy-detrimental genes such as *ADAMTS9* and *FN1* contributing to ZIKV-associated congenital defects.

Currently, all epidemic strains of disease-associated ZIKV belong to the Asian lineage[55]. Our data demonstrate a stark contrast in blood immunity elicited after infection with different lineage ZIKV strains, especially during pregnancy. Specifically, Asian-lineage ZIKV infection led to the profound expansion of non-classical monocytes, an M2-skewed immunosuppressive phenotype of infected monocytes and the aberrant expression of pregnancy-detrimental genes. Although this study provides a better understanding of how Asian ZIKV manipulates the host immunity, which ultimately leads to adverse pregnancy outcomes, it does not negate the role of the inflammatory properties induced by the African ZIKV infection. The robust induction of CXCL10-associated M1 inflammatory responses during the African ZIKV infection resembles many acute inflammatory conditions, such as those seen in infections with the West Nile virus[56] and Japanese encephalitis virus[57]. In a healthy pregnancy, M1 polarization occurs in the third trimester prior to full-term birth[11]. Overt inflammation during the early-to-mid stages of pregnancy can lead to pre-term birth[58]. Thus, this suggests the possibility of complicated pregnancy outcomes regardless of African or Asian ZIKV infection. In summary, our study identified the primary cellular target of ZIKV in the human blood and characterized the heightened sensitivity of maternal monocytes to this virus during pregnancy. This potentially brings new directions for additional immunological studies of ZIKV-infection-induced host immunity during pregnancy, which should be instrumental to develop future therapeutic interventions for improved pregnancy and fetal outcomes.

Methods

Human subjects and blood collection. Peripheral blood specimens were obtained from healthy donors aged 18 to 39 years old and stored temporarily at 37 °C in lithium heparin-containing tube (BD) prior to infection. Blood specimens used in Figures 1–3 were obtained from male and female subjects of equal distribution. Pregnant subjects were recruited at Los Angeles County (LAC) + University of Southern California (USC) Medical Center, with the following exclusion criteria: (i) vaccination within last 14 days, (ii) suspected/recent illness within last 14 days, (iii) steroid administration during pregnancy, (iv) immunodeficiency/immunocompromised conditions, (v) autoimmune disorders, and (vi) suspected fetal anomalies. Pregnancy was categorized into three trimesters based on the following: first trimester < 12 weeks, second trimester 12–28 weeks and third trimester > 28 weeks. Blood serum specimens from 30 symptomatic ZIKV⁺ pregnant women, 10 from each trimester, were collected from pregnant women who were admitted to the acute febrile illness clinic at the Oswaldo Cruz Foundation exhibiting rash that had developed within the previous 5 days. All patients were confirmed to be ZIKV-positive following the performance of reverse transcription-PCR (qRT-PCR) assay in blood or urine which utilized specific probe and primers for ZIKV detection[59]. Serum aliquots from these patients were stored at −80 °C until the performance of the present experiments. Written and oral informed consents were obtained prior to the collection of whole blood, sera and urine specimens from healthy individuals and ZIKV⁺ pregnant patients, and study protocols were approved by institutional review boards of the USC Institutional Review Board (IRB), Fundação Oswaldo Cruz (Fiocruz) and the University of California, Los Angeles (UCLA).

Viruses. African ZIKV strains MR766 (Uganda, 1947) and IbH30656 (Nigeria, 1968), as well as Asian ZIKV strain PRVABC59 (Puerto Rico, 2015) virus stocks were purchased from ATCC. Asian ZIKV strain H/PF/2013 (French Polynesia, 2013) was kindly provided by Dr. Michael Diamond (Washington University School of Medicine). All ZIKV virus stocks were propagated in Vero cell line (ATCC CCL-81, ATCC) and supernatant was harvested at 3–5 dpi. The viral titers were determined by plaque assays on Vero cells. Vero cells were authenticated by morphology check and growth curve analysis, and validated to be mycoplasma-free using Hoechst staining.

In vitro whole blood infection and PBMCs/plasma isolation. Anti-coagulated whole blood specimens were diluted in equal volume of serum-free RPMI (Gibco) prior to ZIKV infection at MOI 0.1 or 1. PBMCs count per ml of whole

blood per donor was counted prior to infection with the appropriate amount of virus. Blood specimens were incubated at 37 °C with intermittent shaking for 24 or 40 hpi. Isolation of PBMCs or plasma were performed by density gradient centrifugation using SepMate (STEMCELL) and lymphocyte separation medium (Corning). Plasma specimens were collected and stored at −80 °C prior to use. PBMCs were further processed for RNA extraction, FACS staining or cell sorting. In this study, total cell population rather than sorted ZIKV⁺ cells were used for all downstream analyses, and were generally termed as "ZIKV/MR766/H/PF2103-infected" specimens.

Flow cytometry and cell sorting. Surface staining of PBMCs were performed with the following antibodies: CD45-BV421 (clone HI30, Biolegend), CD14-AF488 (clone M5E2, Biolegend), CD56-PerCP-Cy5.5 (clone 5.1H11, Biolegend), CD3-AF647 (clone HIT3a, Biolegend) and CD19-PerCP (clone HIB19, Biolegend). PBMCs specimens were either sorted based on surface markers expression using BD LSR III (BD) or proceed on to intracellular ZIKV staining for detection of ZIKV-infected cells. Indirect intracellular ZIKV staining was performed using pan flavivirus antibody (clone D1-4G2-4-15, EMD Millipore), followed by fluorescence-conjugated secondary antibody. For profiling of monocyte subsets, separate surface staining for CD45-BV421, CD14-AF488 and CD16-AF647 (clone 3G8, Biolegend) were performed on PBMCs. All fluorescence-conjugated antibodies were purchased from Biolegend. FACS acquisitions were performed on BD FACSCanto II (BD), using BD FACSDIVA software. All FACS data was analyzed using FlowJo software.

RNA extraction, viral load and gene expression analyses. Total RNA extractions were performed using RNeasy mini/micro Kit (Qiagen) according to manufacturer's instructions. RNA concentration was determined by NanoDrop 1000 spectrophotometer (Thermo Scientific). Extracted total RNA was reverse-transcribed using iScript cDNA synthesis kit (BIO-RAD) according to the manufacturer's instructions. For viral load detection, specific ZIKV NS1 primers and probe targeting conserved NS1 region across all 4 ZIKV strains (MR766, IbH30656, H/PF/2013 and PRVABC59) were designed. Standard curve (10^1 to 10^8 NS1 copies/µl) was generated using serial dilutions of plasmid expressing MR766 NS1 protein. Viral load and gene expression qRT-PCR were performed with 10 ng of cDNA/well using SsoAdvanced Universal Probe Supermix (BIO-RAD) or iQ SYBR Green Supermix (BIO-RAD), respectively. All qRT-PCR reactions were performed using BIO-RAD CFX96 Touch Real-Time PCR Detection System on 96-well plates. Amount of viral load in specimens were interpolated from standard curve using Prism Graphpad software. All viral load qRT-PCR performed in this study included mock controls in which no CT values could be detected. Gene expression fold change was calculated with the $\Delta\Delta Ct$ method using Microsoft Excel. Briefly, $\Delta\Delta Ct = \Delta Ct(\text{ZIKV-infected}) - \Delta Ct(\text{mock control})$ with $\Delta Ct = Ct(\text{gene-of-interest}) - Ct(\text{housekeeping gene-GAPDH})$. The fold change for each gene is calculated as $2^{-\Delta\Delta Ct}$. All primers and probe sequences used in this study is available upon request.

Pan monocyte isolation and human myeloid gene expression analysis. Total monocyte population was isolated from PBMCs using Pan Monocyte Isolation Kit (Miltenyi Biotec), according to manufacturer's instructions. nCounter assay using Human Myeloid Panel (650 genes) (NanoString Technologies) was performed using 1.5 µl of monocyte lysates in RLT lysis buffer (Qiagen) of ~6500 cells/µl, according to manufacturer's instructions. Gene expression analyses were performed using NanoString nSolver software. Background was eliminated by subtracting mean nCounter counts of negative controls supplied in the kit, across counts of all specimens. Gene expressions were expressed as fold change relative to controls (mock-infected specimens). Genes with fold change > 1.5 is considered to be induced. The NanoString gene analysis data were deposited in the NCBI GEO database under the accession code GSE101718.

Multiplex immunoassay and ELISA. Serum levels of human IL-12 p40, IL-10, sCD163 and YKL-40 were detected using Bio-plex multiplex immunoassay (BIO-RAD). Human CXCL10 and IL-10 ELISA assays (Biolegend) were performed on plasma specimens according to manufacturer's instructions. Human FN1 ELISA assay (LSBio) was performed on serum specimens according to manufacturer's instructions.

Statistical analyses. All statistical analyses were performed using GraphPad Prism 5.0 software. For analyses between 2 groups, Mann-Whitney U test were used. For comparisons among more than 2 groups, either one-way or two-way ANOVA, Bonferroni post-test was used.

Data availability. The data supporting the findings of this study are available in the paper and Supplementary Information. All primers and probe sequences used in this study are available upon request. The NanoString gene analysis data were deposited in the NCBI GEO database (https://www.ncbi.nlm.nih.gov/geo), under the accession code GSE101718.

References

1. Benitez, M. A. Climate change could affect mosquito-borne diseases in Asia. *Lancet* **373**, 1070 (2009).
2. Chouin-Carneiro, T. et al. Differential susceptibilities of *Aedes aegypti* and *Aedes albopictus* from the Americas to Zika virus. *PLoS Negl. Trop. Dis.* **10**, e0004543 (2016).
3. *Zika Situation Report: 20 January 2017* (World Health Organization, 2017).
4. Enfissi, A., Codrington, J., Roosblad, J., Kazanji, M. & Rousset, D. Zika virus genome from the Americas. *Lancet* **387**, 227–228 (2016).
5. Wang, L. et al. From mosquitos to humans: genetic evolution of Zika virus. *Cell Host Microbe* **19**, 561–565 (2016).
6. Simonin, Y. et al. Zika virus strains potentially display different infectious profiles in human neural cells. *EBioMedicine* **12**, 161–169 (2016).
7. Jurado, K. A. et al. Zika virus productively infects primary human placenta-specific macrophages. *JCI Insight* **1**, e88461 (2016).
8. Noronha, L., Zanluca, C., Azevedo, M. L., Luz, K. G. & Santos, C. N. Zika virus damages the human placental barrier and presents marked fetal neurotropism. *Mem. Inst. Oswaldo Cruz* **111**, 287–293 (2016).
9. Racicot, K., Kwon, J. Y., Aldo, P., Silasi, M. & Mor, G. Understanding the complexity of the immune system during pregnancy. *Am. J. Reprod. Immunol.* **72**, 107–116 (2014).
10. Faas, M. M., Spaans, F. & De Vos, P. Monocytes and macrophages in pregnancy and pre-eclampsia. *Front. Immunol.* **5**, 298 (2014).
11. Brown, M. B., von Chamier, M., Allam, A. B. & Reyes, L. M1/M2 macrophage polarity in normal and complicated pregnancy. *Front. Immunol.* **5**, 606 (2014).
12. Wong, K. L. et al. The three human monocyte subsets: implications for health and disease. *Immunol. Res.* **53**, 41–57 (2012).
13. Shechter, R., London, A. & Schwartz, M. Orchestrated leukocyte recruitment to immune-privileged sites: absolute barriers versus educational gates. *Nat. Rev. Immunol.* **13**, 206–218 (2013).
14. Audoy-Rémus, J. et al. Rod-shaped monocytes patrol the brain vasculature and give rise to perivascular macrophages under the influence of proinflammatory cytokines and angiopoietin-2. *J. Neurosci.* **28**, 10187–10199 (2008).
15. Kourtis, A. P., Read, J. S. & Jamieson, D. J. Pregnancy and infection. *N. Engl. J. Med.* **370**, 2211–2218 (2014).
16. Mantovani, A. et al. The chemokine system in diverse forms of macrophage activation and polarization. *Trends Immunol.* **25**, 677–686 (2004).
17. Martinez, F. O. & Gordon, S. The M1 and M2 paradigm of macrophage activation: time for reassessment. *F1000Prime Rep.* **6**, 13 (2014).
18. Murray, P. J. & Wynn, T. A. Protective and pathogenic functions of macrophage subsets. *Nat. Rev. Immunol.* **11**, 723–737 (2011).
19. Jaguin, M., Houlbert, N., Fardel, O. & Lecureur, V. Polarization profiles of human M-CSF-generated macrophages and comparison of M1-markers in classically activated macrophages from GM-CSF and M-CSF origin. *Cell Immunol.* **281**, 51–61 (2013).
20. Magatti, M. et al. Human amnion favours tissue repair by inducing the M1-to-M2 switch and enhancing M2 macrophage features. *J. Tissue Eng. Regen. Med.* **10**, 2193 (2016).
21. Mack, I. et al. The role of chitin, chitinases, and chitinase-like proteins in pediatric lung diseases. *Mol. Cell Pediatr.* **2**, 3 (2015).
22. Martines, R. B. Notes from the field: evidence of Zika virus infection in brain and placental tissues from two congenitally infected newborns and two fetal losses—Brazil, 2015. *MMWR* **65**, 159–160 (2016).
23. Sordet, O. et al. Specific involvement of caspases in the differentiation of monocytes into macrophages. *Blood* **100**, 4446–4453 (2002).
24. Saeed, S. et al. Epigenetic programming of monocyte-to-macrophage differentiation and trained innate immunity. *Science* **345**, 1251086 (2014).
25. Brasil, P. et al. Zika virus infection in pregnant women in Rio de Janeiro—preliminary report. *N. Engl. J. Med.* **375**, 2321–2334 (2016).
26. Brasil, P. et al. Zika virus infection in pregnant women in Rio de Janeiro. *N. Engl. J. Med.* **375**, 2321–2334 (2016).
27. Ishida, J. et al. Pregnancy-associated homeostasis and dysregulation: lessons from genetically modified animal models. *J. Biochem.* **150**, 5–14 (2011).
28. Bruchova, H. et al. Effect of maternal tobacco smoke exposure on the placental transcriptome. *Placenta* **31**, 186–191 (2010).
29. Chaemsaithong, P. et al. Characterization of the myometrial transcriptome in women with an arrest of dilatation during labor. *J. Perinat. Med.* **41**, 665–681 (2013).
30. Chen, C. K. et al. Fibronectin levels in normal pregnancy and preeclampsia. *J. Formosan Med. Assoc.* **93**, 921–924 (1994).
31. Rasanen, J. et al. Maternal serum glycosylated fibronectin as a point-of-care biomarker for assessment of preeclampsia. *Am. J. Obstet. Gynecol.* **212**, 82.e1–82.e9 (2015).
32. Melo, A. S. et al. Congenital Zika virus infection: beyond neonatal microcephaly. *JAMA Neurol.* **73**, 1407–1416 (2016).
33. Parra, B. et al. Guillain–Barré syndrome associated with Zika virus infection in Colombia. *N. Engl. J. Med* **375**, 1513–1523 (2016).
34. Waggoner, J. J. & Pinsky, B. A. Zika virus: diagnostics for an emerging pandemic threat. *J. Clin. Microbiol.* **54**, 860–867 (2016).
35. Rossi, S. L. et al. Characterization of a novel murine model to study Zika virus. *Am. J. Trop. Med. Hyg.* **94**, 1362–1369 (2016).
36. Delaloye, J. et al. Innate immune sensing of modified vaccinia virus Ankara (MVA) is mediated by TLR2-TLR6, MDA-5 and the NALP3 inflammasome. *PLoS Pathog.* **5**, e1000480 (2009).
37. Her, Z. et al. Active infection of human blood monocytes by Chikungunya virus triggers an innate immune response. *J. Immunol.* **184**, 5903–5913 (2010).
38. Hou, W. et al. Viral infection triggers rapid differentiation of human blood monocytes into dendritic cells. *Blood* **119**, 3128–3131 (2012).
39. Osuna, C. E. et al. Zika viral dynamics and shedding in rhesus and cynomolgus macaques. *Nat. Med.* **22**, 1448–1455 (2016).
40. Teng, T. S. et al. Viperin restricts chikungunya virus replication and pathology. *J. Clin. Invest.* **122**, 4447–4460 (2012).
41. Robinson, T. O., Zhang, M., Ochsenbauer, C., Smythies, L. E. & Cron, R. Q. CD4 regulatory T cells augment HIV-1 expression of polarized M1 and M2 monocyte derived macrophages. *Virology* **504**, 79–87 (2017).
42. Fischer-Smith, T., Tedaldi, E. M. & Rappaport, J. CD163/CD16 coexpression by circulating monocytes/macrophages in HIV: potential biomarkers for HIV infection and AIDS progression. *AIDS Res. Hum. Retroviruses* **24**, 417–421 (2008).
43. Palmer, C. et al. HIV elite controllers have lower frequencies of CD14dimCD16+ inflammatory monocytes with greater CX3CR1-dependent tissue homing potential than viremic controllers (VIR9P. 1138). *J. Immunol.* **194**, 215 (2015).
44. Zonneveld, R. et al. Three atypical lethal cases associated with acute Zika virus infection in Suriname. *IDCases* **5**, 49–53 (2016).
45. Halai, U. A. et al. Maternal Zika virus disease severity, virus load, prior dengue antibodies and their relationship to birth outcomes. *Clin. Infect. Dis* **2017**, 472 (2017).
46. Suy, A. et al. Prolonged Zika virus viremia during pregnancy. *N. Engl. J. Med.* **375**, 2611–2613 (2016).
47. Driggers, R. W. et al. Zika virus infection with prolonged maternal viremia and fetal brain abnormalities. *N. Engl. J. Med.* **374**, 2142–2151 (2016).
48. Hamel, R. et al. Biology of Zika virus infection in human skin cells. *J. Virol.* **89**, 8880–8896 (2015).
49. Miner, J. J. et al. Zika virus infection during pregnancy in mice causes placental damage and fetal demise. *Cell* **165**, 1081–1091 (2016).
50. Melgert, B. N. et al. Pregnancy and preeclampsia affect monocyte subsets in humans and rats. *PLoS ONE* **7**, e45229 (2012).
51. Brooks, D. G. et al. Interleukin-10 determines viral clearance or persistence in vivo. *Nat. Med.* **12**, 1301–1309 (2006).
52. Brooks, D. G., Lee, A. M., Elsaesser, H., McGavern, D. B. & Oldstone, M. B. IL-10 blockade facilitates DNA vaccine-induced T cell responses and enhances clearance of persistent virus infection. *J. Exp. Med.* **205**, 533–541 (2008).
53. Redpath, S., Ghazal, P. & Gascoigne, N. R. Hijacking and exploitation of IL-10 by intracellular pathogens. *Trends Microbiol.* **9**, 86–92 (2001).
54. Ornelas, A. M. et al. Immune activation in amniotic fluid from Zika virus-associated microcephaly. *Ann. Neurol.* **81**, 152–156 (2017).
55. Zhu, Z. et al. Comparative genomic analysis of pre-epidemic and epidemic Zika virus strains for virological factors potentially associated with the rapidly expanding epidemic. *Emerg. Microbes Infect.* **5**, e22 (2016).
56. Klein, R. S. et al. Neuronal CXCL10 directs CD8+ T-cell recruitment and control of West Nile virus encephalitis. *J. Virol.* **79**, 11457–11466 (2005).
57. Bhowmick, S. et al. Induction of IP-10 (CXCL10) in astrocytes following Japanese encephalitis. *Neurosci. Lett.* **414**, 45–50 (2007).
58. Challis, J. R. et al. Inflammation and pregnancy. *Reprod. Sci.* **16**, 206–215 (2009).
59. Lanciotti, R. S. et al. Genetic and serologic properties of Zika virus associated with an epidemic, Yap State, Micronesia, 2007. *Emerg Infect Dis.* **14**, 1232–1239 (2008).

Author contributions

S.-S.F. performed and analysed all the experiments, prepared the figures and wrote the first draft of the manuscript. W.C., Y.C., J.W.B., L.-C.C., Y.C.,

J.S.Y., J.G., G.C., A.B., K.N.S. and P.B. collaborated for the experimental design and interpretation. S.-S.F. and J.U.J. jointly conceived the experimental design, interpreted the results and wrote subsequent drafts of the manuscript.

Competing interests

The authors declare no competing financial interests.

Additional information